ISSN 0007-2621

B K

No. 4 1978

issued quarterly

Technical Review

To Advance Techniques in Acoustical, Electrical and Mechanical Measurement

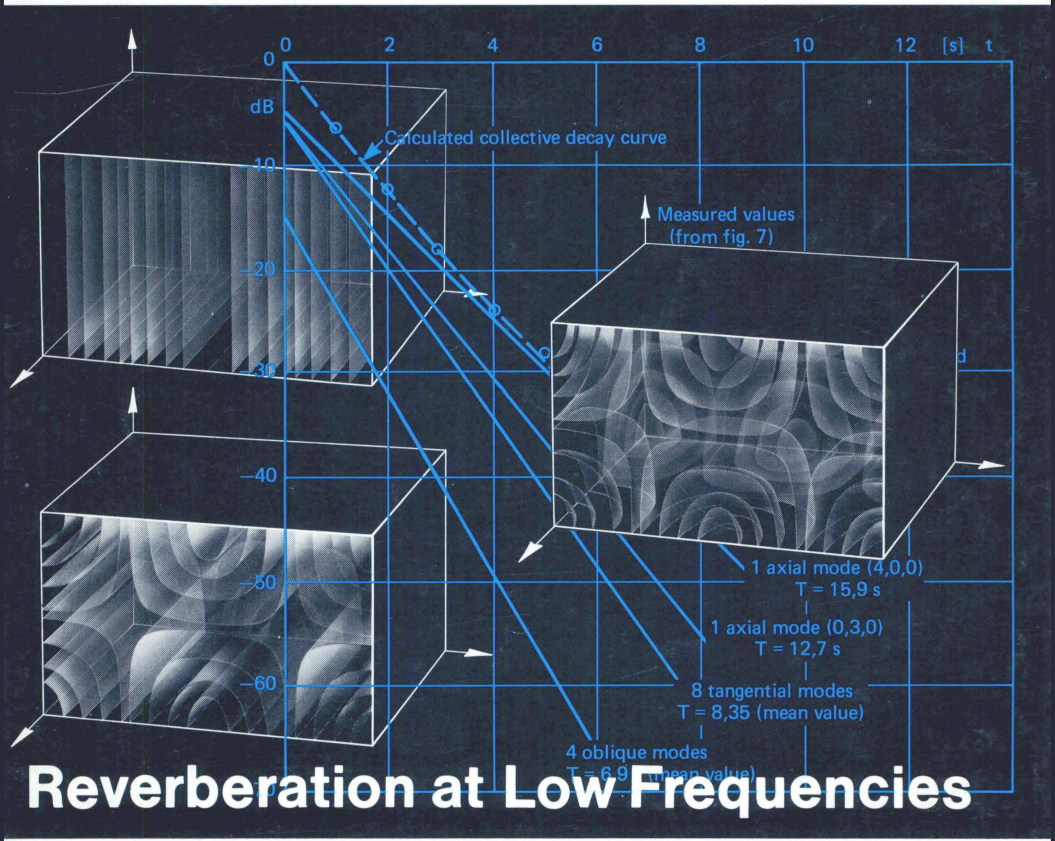

Reverberation at Low Frequencies

Brüel & Kjær

PREVIOUSLY ISSUED NUMBERS OF BRÜEL & KJÆR TECHNICAL REVIEW

3–1978 The Enigma of Sound Power Measurements at Low Frequencies.

2–1978 The Application of the Narrow Band Spectrum Analyzer Type 2031 to the Analysis of Transient and Cyclic Phenomena.
Measurement of Effective Bandwith of Filters.

1–1978 Digital Filters and FFT Technique in Real-time Analysis.

4–1977 General Accuracy of Sound Level Meter Measurements.
Low Impedance Microphone Calibrator and its Advantages.

3–1977 Condenser Microphones used as Sound Sources.

2–1977 Automated Measurements of Reverberation Time using the Digital Frequency Analyzer Type 2131.
Measurement of Elastic Modulus and Loss Factor of PVC at High Frequencies.

1–1977 Digital Filters in Acoustic Analysis Systems.
An Objective Comparison of Analog and Digital Methods of Real-Time Frequency Analysis.

4–1976 An Easy and Accurate Method of Sound Power Measurements.
Measurement of Sound Absorption of rooms using a Reference Sound Source.

3–1976 Registration of Voice Quality.
Acoustic Response Measurements and Standards for Motion-Picture Theatres.

2–1976 Free-Field Response of Sound Level Meters.
High Frequency Testing of Gramophone Cartridges using an Accelerometer.

1–1976 Do We Measure Damaging Noise Correctly?

4–1975 On the Measurement of Frequency Response Functions.

3–1975 On the Averaging Time of RMS Measurements (continuation).

2–1975 On the Averaging Time of RMS Measurements
Averaging Time of Level Recorder Type 2306 and "Fast" and "Slow" Response of Level Recorders 2305/06/07

1–1975 Problems in Telephone Measurements.
Proposals for the Measurement of Loudness Ratings of Operators' Headsets.
Comparison of Results obtained by Subjective Measuring Methods.
Repeatabilities in Electro-Acoustic Measurements on Telephone Capsules.
Stable Subset Measurements with the 73 D
Vibration Testing of Telephone Equipment.

(Continued on cover page 3)

TECHNICAL REVIEW

No. 4 — 1978

Contents

Reverberation Process at Low Frequencies

by

Holger Larsen

ABSTRACT

The reverberation process in a rectangular room was investigated using sophisticated instrumentation. By averaging many reverberation decays it was possible to determine the decay curves free of interference allowing the details to be seen. The decay curves measured show some curvature especially at low frequencies and as a result there are discrepancies between reverberation times determined from the early decay rate and from those determined from the slope between —5 and —35 dB, as suggested by ISO Standards 354 and 3382.

The reverberation process for a frequency band is the result of the decays of the normal modes in the band, each mode decaying with its own time constant which depends essentially on the mean free path between reflections. A formula for the mean free path is derived and hence a formula for the decay curve is also derived. Good agreement was obtained between the measured and calculated decay curves.

SOMMAIRE

Le processus de réverbération dans une pièce rectangulaire a été étudié au moyen d'instruments de mesure sophistiqués. L'intégration de nombreuses courbes de réverbération permet de déterminer une courbe d'amortissement libre de toute interférence à partir de laquelle on peut examiner les détails. Les courbes d'amortissement mesurées présentent une courbure particulièrement aux basses fréquences et ceci conduit à des écarts entre les temps de réverbération déterminés à partir de la pente à l'origine et ceux déterminés à partir de la pente entre —5 et —35 dB,omme le suggèrent les normes ISO 354 et 3382.

Le processus de réverbération pour une bande de fréquence donnée est le résultat de l'amortissement des modes propres dans cette bande de fréquence, chaque mode s'amortissant avec sa propre constante de temps, laquelle dépend essentiellement du libre parcours moyen entre les réflections. On déduit une formule donnant le libre parcours moyen et, de là, une formule donnant la courbe d'amortissement. La corrélation entre les courbes d'amortissement mesurées et calculées s'est avérée bonne.

ZUSAMMENFASSUNG

Mit einem anspruchsvollen Meßaufbau wurde der Abklingvorgang von Schall in einem quaderförmigen Raum untersucht. Durch die Mittelung über viele Nachhallmessungen war es möglich, eine Abklingkurve zu ermitteln, bei der der Einfluß von Interferenzen unterdrückt ist, und Einzelheiten sind erkennbar. Die gemessenen Abklingkurven zeigen eine gewisse Krümmung, speziell bei tiefen Frequenzen, und als Ergebniss erhielt man unterschiedliche Nachhallzeiten, wenn am Beginn der Abklingkurve und im Bereich zwischen —5 und —35 dB, wie in ISO 354 und 3382 empfohlen, gemessen wird.
Der Nachhallvorgang für jedes Frequenzband ist das Ergebniss vom Abklingen der Eigenfrequenzen in diesem Frequenzband, welche jede mit ihrer eigenen Zeitkonstante abfällt die im wesentlichen von der mittleren freien Weglänge zwischen den Reflektionen abhängt. Eine Formel für die mittlere freie Weglänge wird entwickelt und daraus eine für die Nachhallkurve. Zwischen der errechneten Kurve und praktischen Messungen zeigten sich gute Übereinstimmungen.

Introduction

Reverberation time is an important factor in assessing the acoustic quality of a room. It is also used in the determination of isolation, absorption, and sound power. Reverberation time for a given frequency band is defined as the time required for the average sound pressure level, originally in the steady state, to decrease 60 dB after the source is stopped. Although there are several methods by which it can be determined, the classical method, where the sound pressure level decay is registered on a level recorder, is still the most common and is also standardised in ISO 354 and 3382 Ref.[1, 2]. It is assumed in these standards that the decay rate is exponential and therefore manifests itself as a straight line when the sound pressure level is represented on a logarithmic scale. However, on account of the interferences between the individual eigenmodes the curve traced out is not smooth, especially at low frequencies where the number of eigenmodes are relatively few. Fig.1 shows typical examples of decay curves at low frequencies. According to the standards the reverberation time is determined from the slope of a line drawn on the decay curve between —5 dB and —35 dB levels below the steady state level. To improve the accuracy an average value is determined from a number of curves obtained with different microphone and source positions.

At low frequencies, however, the sound pressure does not often decay exponentially and the decay curve deviates from a straight line on a logarithmic plot. Several authors [3, 4] have investigated this phenomenon theoretically, where it is shown that the slope at the start of the decay curve (early decay rate) is numerically highest and reduces as the level decreases. It has been difficult to substantiate the theoretical treatment with practical measurements upto the present day on account of the uneveness of the curves mentioned above.

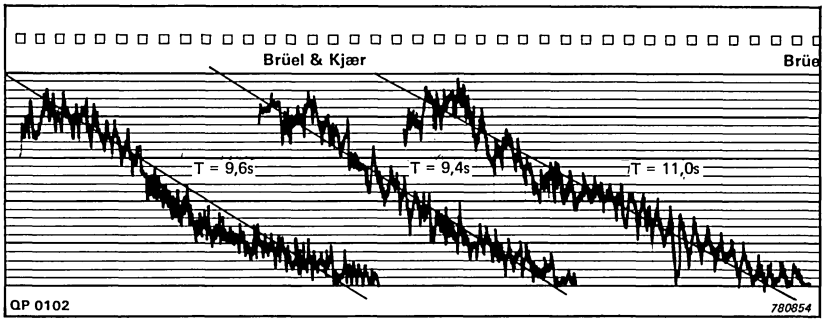

Fig.1. Examples of 100 Hz 1/3 octave band decay curves using the classical method. The same measurement repeated three times

Today, however, sophisticated instrumentation and new methods have been developed which permit reverberation time measurements to be carried out with a much higher degree of accuracy. Such a measurement method which makes use of a digital real time parallel analyzer and a desk-top calculator is described in Technical Review No.2—1977 [5]. The purpose of this article is to illustrate this method with some measurement results and analyze the reverberation process at *low* frequencies.

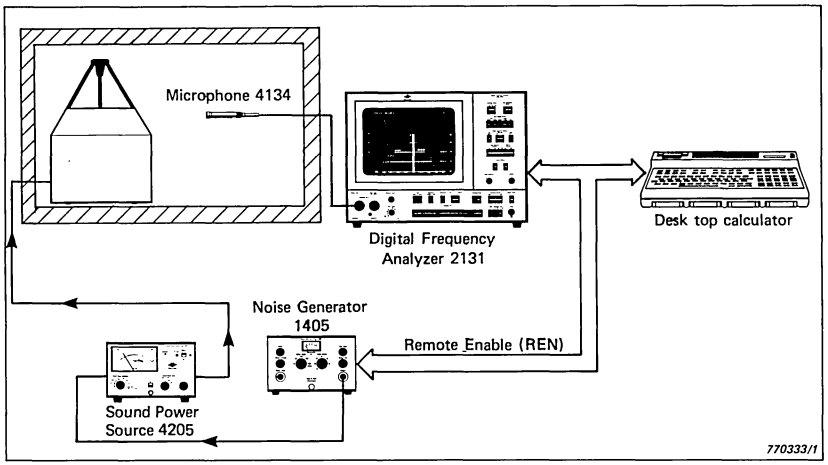

Fig.2. Automatic system for reverberation time measurements

Measurement Method

Fig.2 shows an instrumentation set-up for automatic measurement of reverberation time. The system is controlled remotely by the desk-top calculator and operates after the following procedure: the Noise Generator Type 1405 is started and sends a pink noise signal to the Sound Power Source Type 4205 which is used here as a power amplifier for the loudspeaker Type HP 1001. After a steady state sound field is built-up in the room, a signal to the Digital Frequency Analyzer Type 2131 starts recording of the spectra over short time intervals and soon after the sound source is stopped, see Fig.3. During each time interval the frequency spectra are recorded over a selected averaging time and the averaged spectrum then readout to the desk-top calculator and stored. (Each time interval is made up of an averaging time plus read-out time).

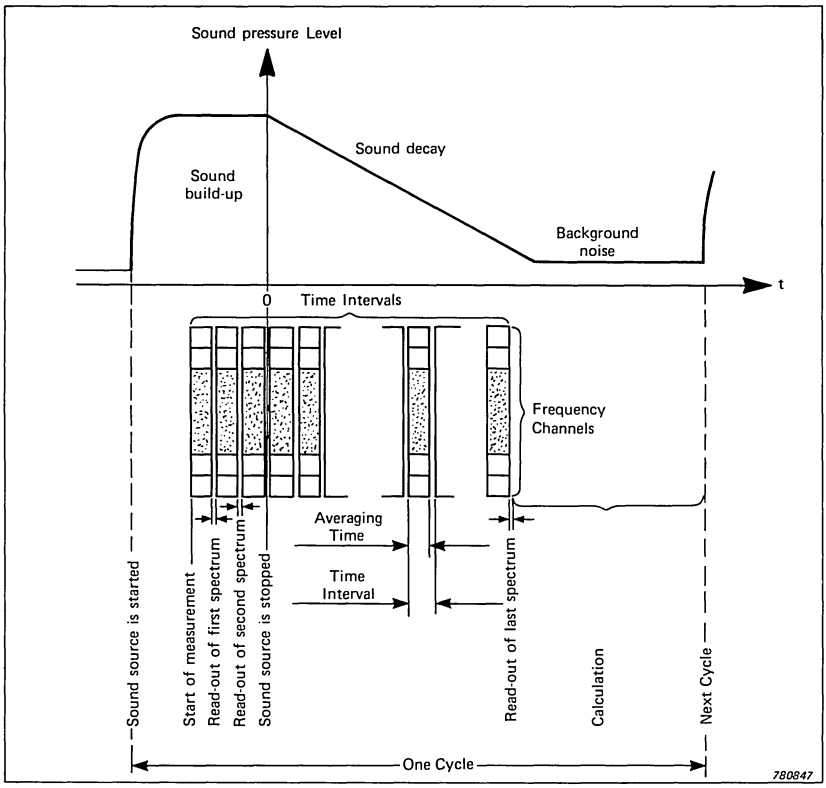

Fig.3. Time history for one measurement cycle

Time Interval	Averaging Time	
ms	s	ms
44	1/32	31,25
66 – 110	1/16	62,5
132 – 242	1/8	125
264 – 484	1/4	250

790103

Table 1

The shortest time interval that can be chosen is 44 ms. Larger time intervals can be chosen (depending on the averaging time see Table 1) in steps of 44 + n.22 where n is an integer. After the spectra have been recorded and read-out for a maximum of 65 time intervals and time allowed for calculation, the sound source is started again and the cycle repeated. The time taken for each cycle is between 40 and 60 s depending on the chosen parameters. The cycle is repeated as many times as desired after which the average level in each of the time intervals for each frequency band is calculated.

The reverberation time may now be evaluated using the calculator for each frequency band or the average levels in each time interval can be fed to a level recorder and the reverberation time evaluated from the slope of the curves for each frequency band.

For the measurements a reverberation room in the Acoustics Laboratory at the Danish Technical University (D.T.H.) was used.

Twenty diffusors of area 1,2 × 0,9 m^2 were installed in the room the dimensions of which are given in Table 2.

Length	m	7,85
Width	m	6,25
Height	m	4,95
Volume	m^3	243
Surface area (without diffusers)	m^2	238
Number of diffusers		20
Surface area of diffusers	m^2	0,9 x 1,2

790104

Table 2

Measurement Results

a) Measurements with stationary source and microphone positions
The microphone and source positions are shown in Fig.4. For source position A measurements were carried out for all the microphone positions while for position B only microphone positions 1, and 2 were used. Figs.5a and b show reverberation curves plotted on a level recorder chart for 1/3 octave frequency bands of centre frequencies 80 Hz and 160 Hz respectively, for different source and microphone positions. Values of 600 spectra have been averaged for each time interval which was chosen to be 110 ms.

It can be seen from the figures that the random fluctuations of the curves have disappeared on account of averaging over a large number of spectra. But the curves still show some irregularity, the magnitude of which depends on the source and microphone positions. The irregularities would seem to be due to the interference between the eigenmodes with slight differences in the resonant frequencies.

The problem of interference could be avoided if spatial averaging, in addition to the time averaging was also carried out. In other words, the level in each time interval would be averaged over a number of spectra and over a number of source and microphone positions. To try this out further measurements were taken with a rotating microphone whilst revolving the source in the room.

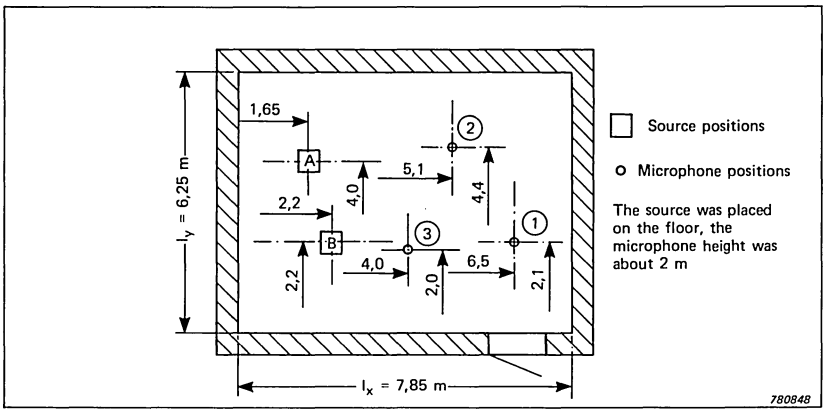

Fig.4. Stationary source and microphone positions for reverberation time measurements

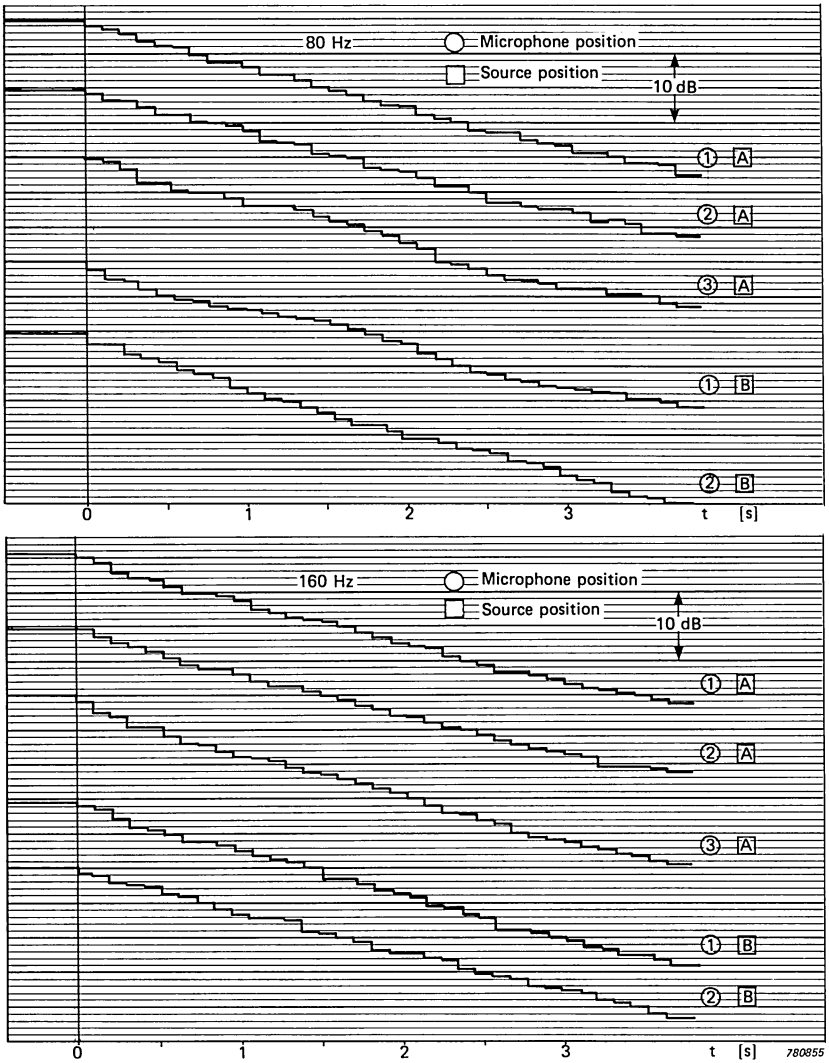

Fig.5. Decay curves for stationary sound source and microphone positions. Time interval 110 ms.
a. 80 Hz 1/3 octave band.
b. 160 Hz 1/3 octave band.

b) Measurements with rotating microphone and sound source

Fig.6 shows a measurement set-up where the sound source is mounted on the end of a wooden beam fixed to a Turntable Type 3922. The sound source was rotated in a circle of radius approx. 2 m with a rotation time of 80 s. The Microphone Boom Type 3923 was used for rotating the microphone in a circle of radius 1,5 m and rotation time 64 s.

The reverberation curves obtained using the instrumentation described above are shown in Figs.7a and b. It can be seen that the curves are regular (due to the absence of interferences) but with some curvature which is especially noticeable for low frequencies. In each time interval of 110 ms the levels have been averaged over approx. 1600 cycles, and as each cycle takes about 1 minute the total measurement time involved was approx. 27 hours.

From the decay curves in Fig.7 the reverberation times T have been evaluated according to ISO standard 354 by using the slope of the curves between the —5 dB and —35 dB levels. The reverberation times evaluated from the slope of the early decay rate are designated by T_e.

Fig.6. Measuring set-up for rotating sound source and microphone

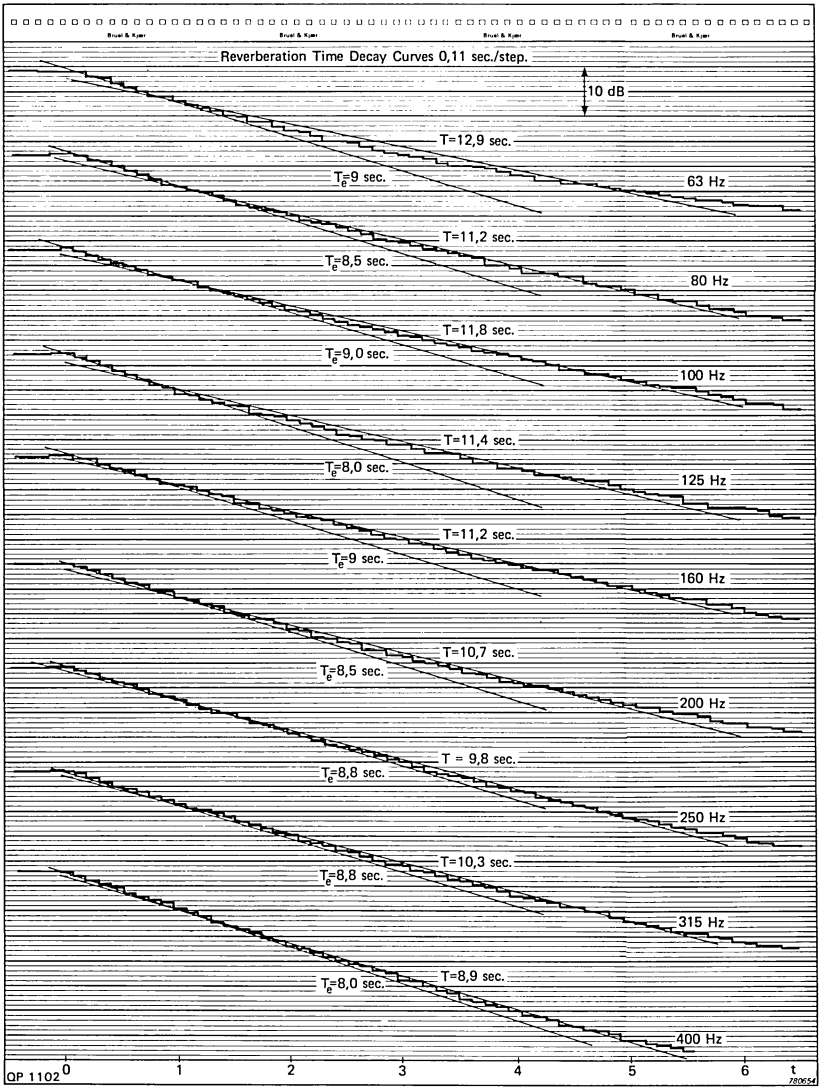

Fig. 7a. Decay curves for rotating sound source and microphone. Time interval 110 ms.
1/3 octave band centre frequencies 63 Hz — 400 Hz

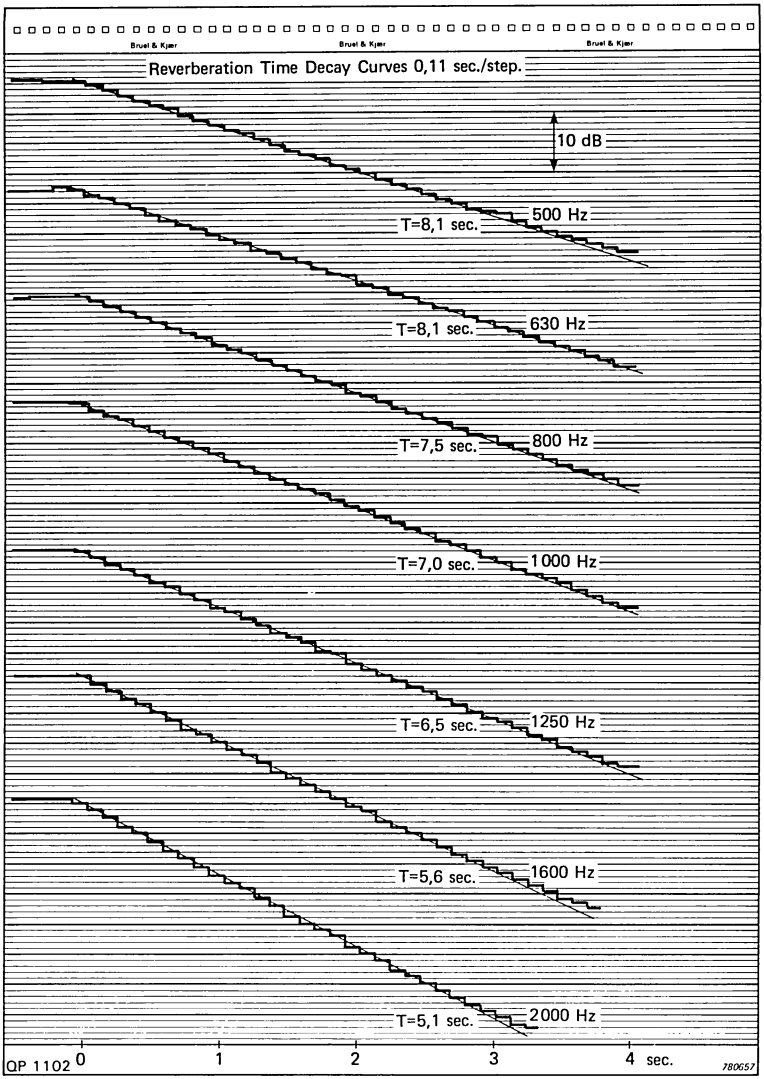

Fig. 7b. Decay curves for rotating sound source and microphone Time interval 110 ms.
1/3 octave band centre frequencies 500 Hz — 2000 Hz

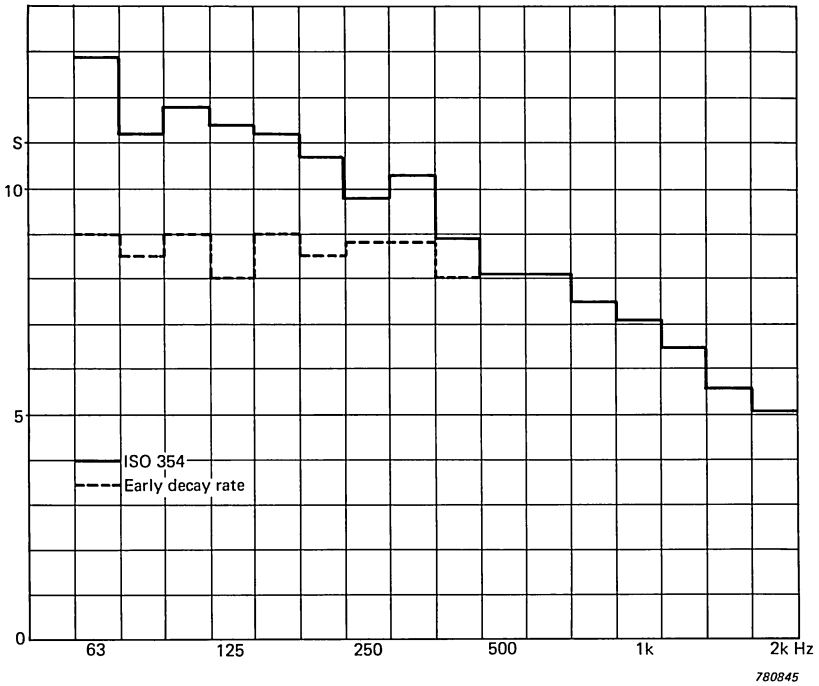

Fig.8. Reverberation time measured according to ISO 354 (—5 to —35 dB) and early decay rate calculated from curves in Fig.7. Time interval 110 ms

Both T and T_e are plotted against frequency in Fig.8 and it can be seen that T_e is much lower than T for low frequencies.

In order to examine the early decay rate of the reverberation process in greater detail, further measurements were taken with a time interval of 44 ms instead of 110 ms. The levels in each time interval were again averaged over 1600 cycles. Fig.9 shows the reverberation curves while in Fig.10 the early decay rates obtained for 44 ms and 110 ms time intervals are compared.

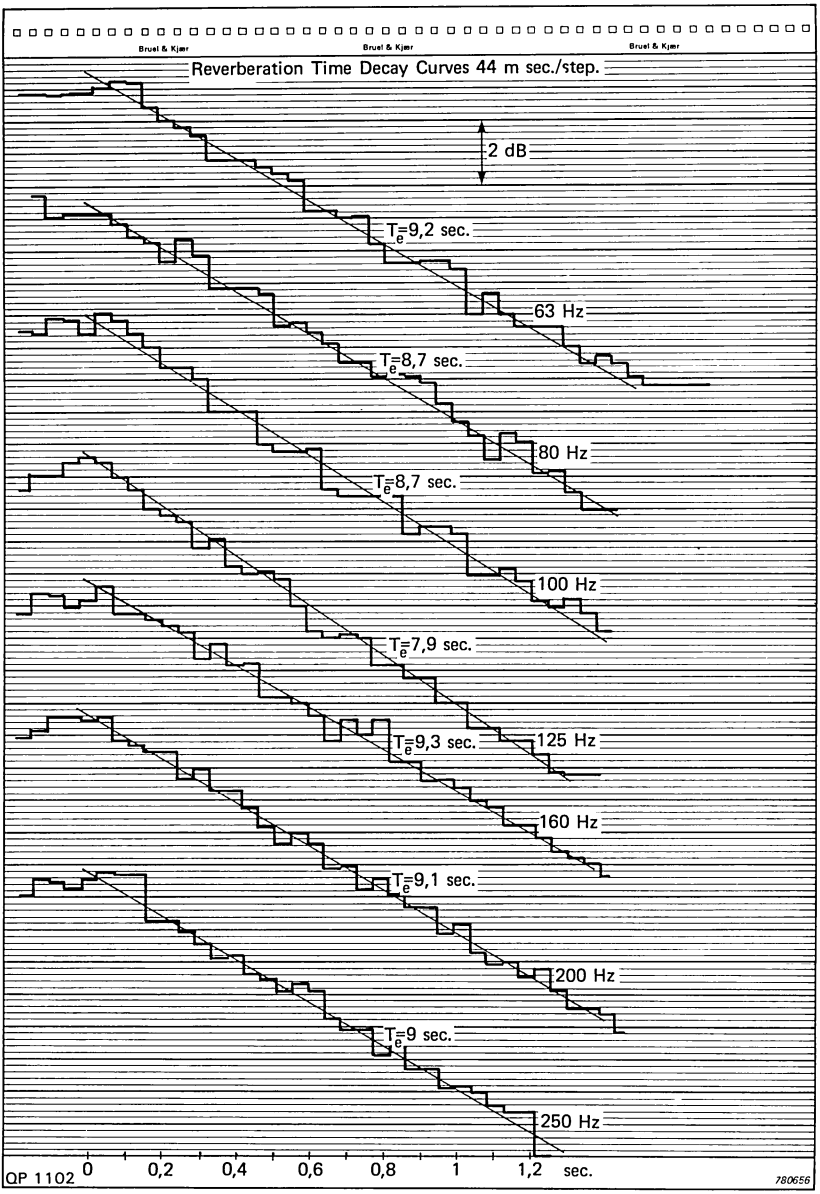

Fig.9. Decay curves for rotating sound source and microphone. Time interval 44 ms

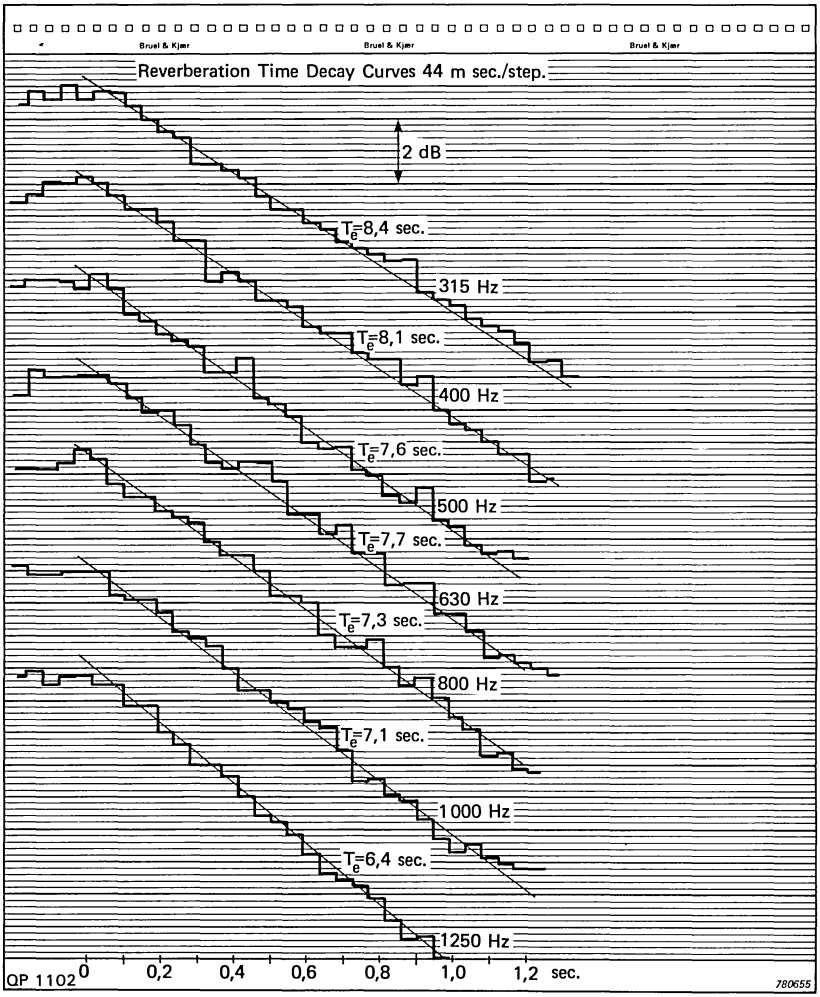

Fig.9. Continued

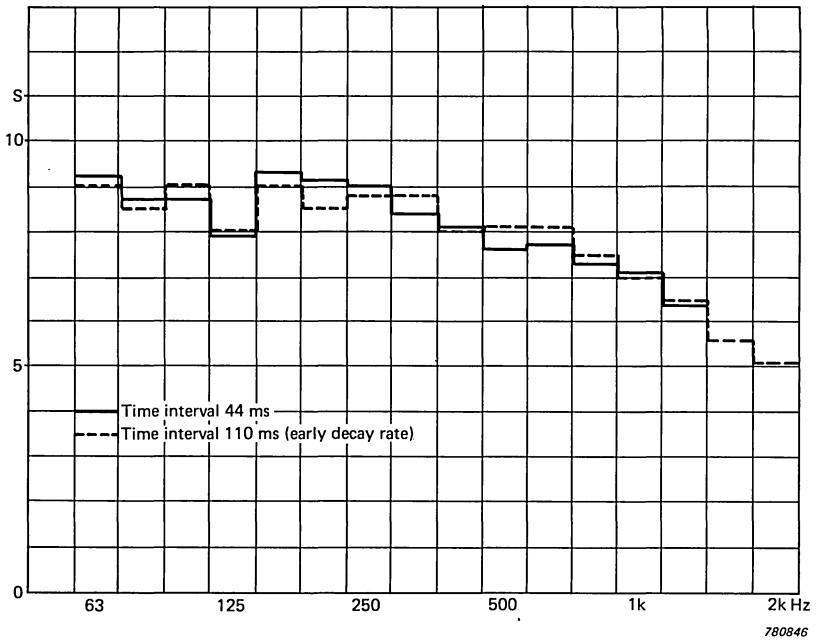

Fig.10. Reverberation time measured using a time interval 44 ms compared to measurements using 110 ms

Sound Pressure, Particle Velocity and Energy Density Distribution in a Room

When a sound source is operated in a room, a number of different room resonances (sometimes referred to as normal modes or eigenmodes) are excited. The type of eigenmode excited depends on how the initial wave is reflected and returns to the point of excitation in the same phase and direction as the initial wave. In a rectangular room the simplest eigenmode is the *axial* mode in which the component waves travel along one axis (one dimensional) parallel to two wall pairs as shown in Fig.11a. The sound pressure in the room varies as shown by the curve in the Figure. It can be seen that when a moving microphone is used, the RMS value of the sound pressure in the room will be measured which is $\sqrt{2}$ times lower than the values at the points of maxima. The sound pressure variation in the room can also be illustrated by drawing lines through points of equal pressures. As shown in Fig.11b these points lie in planes for axial waves.

Fig.11c shows planes formed by points of equal particle velocities and

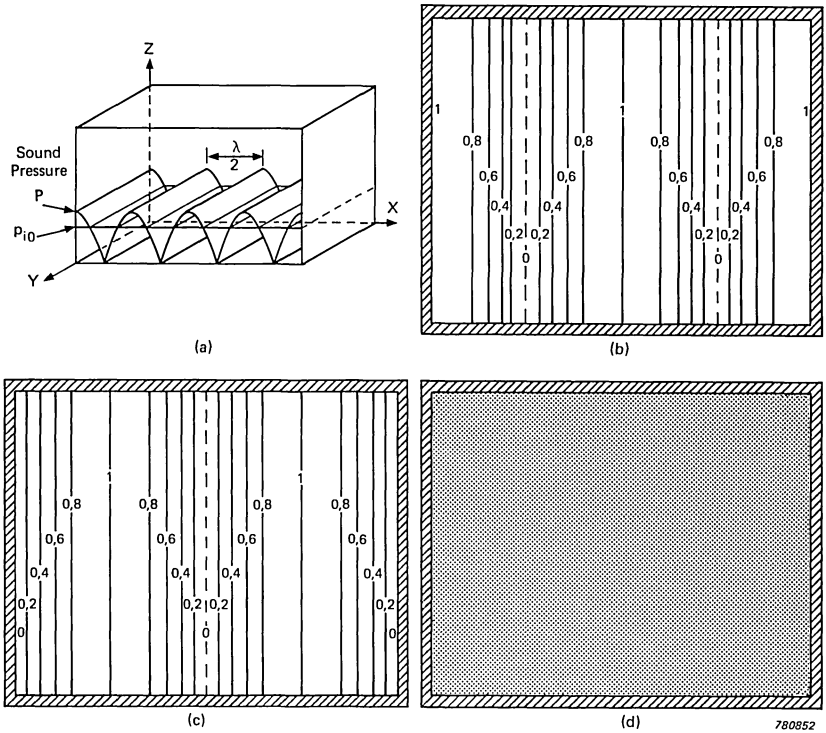

Fig.11. Sound distribution in a rectangular room for an axial mode. Values are normalized to maximum effective sound pressure P.
a. Sound pressure pattern, mode (4,0,0)
b. Sound pressure contours on a section through the room, mode (2,0,0)
c. Particle velocity contours, mode (2,0,0)
d. Energy density contours, mode (2,0,0). For an axial mode the energy density is uniform

it can be seen that the planes with maximum pressures occur at the points of zero particle velocity and vice versa.

The energy density is uniform all over the room as shown in Fig.11d for axial waves. At any point in the room the energy density is obtained by determining the sum of the squares of the normalised values given in Figs.11b and c. The mathematical derivation of the values shown in these figures is given in Appendix A.

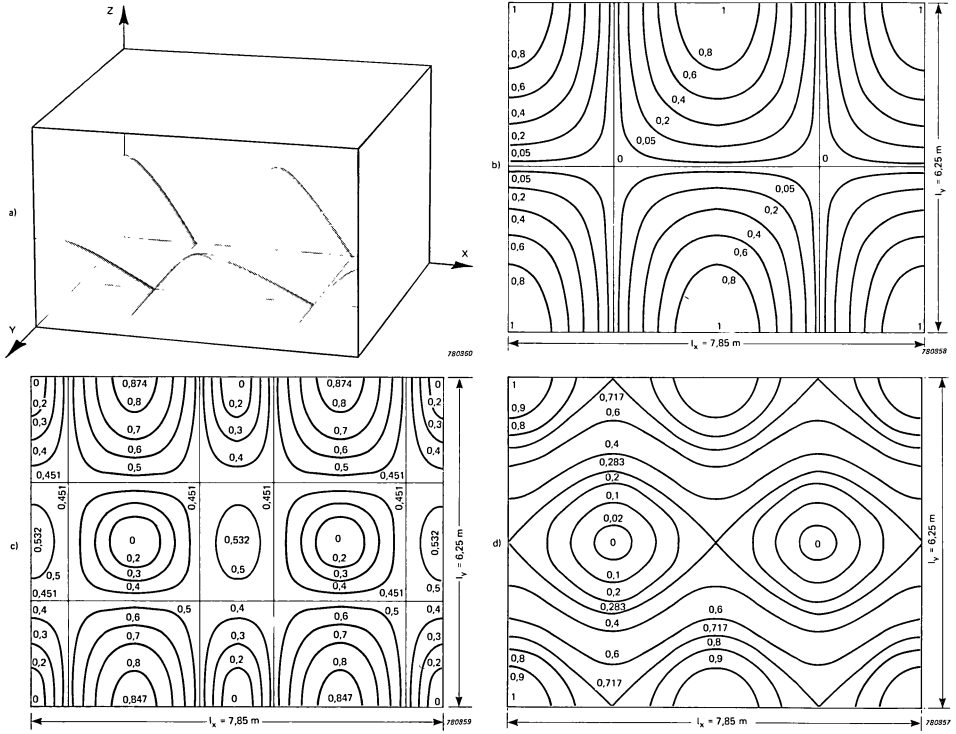

Fig. 12. Sound distribution in a rectangular room for the tangential mode (2,1,0). Values are normalized to maximum effective sound pressure a. Sound pressure pattern b. Sound pressure contours on a section through the room c. Particle velocity contours d. Energy density contours

Another type of eigenmode is one in which the component waves are parallel to one pair of walls but are oblique to the other two pairs (two dimensional) and is termed a *tangential* mode, Fig.12a. Figs12b, c and d show surfaces with constant pressure, particle velocity and energy density for a tangential mode. It can be seen from Figs.11 and 12 that for a tangential mode, in contrast to an axial mode, there are points in the room where the sound pressure, particle velocity, and energy density are all zero.

The third type of an eigenmode is one in which the component waves are parallel to none of the three wall pairs and is termed an *oblique* mode. Fig.13 shows surfaces with constant pressure for an oblique mode. As for the tangential modes, the oblique modes have points in the room where the sound pressure, particle velocity and energy density are all zero.

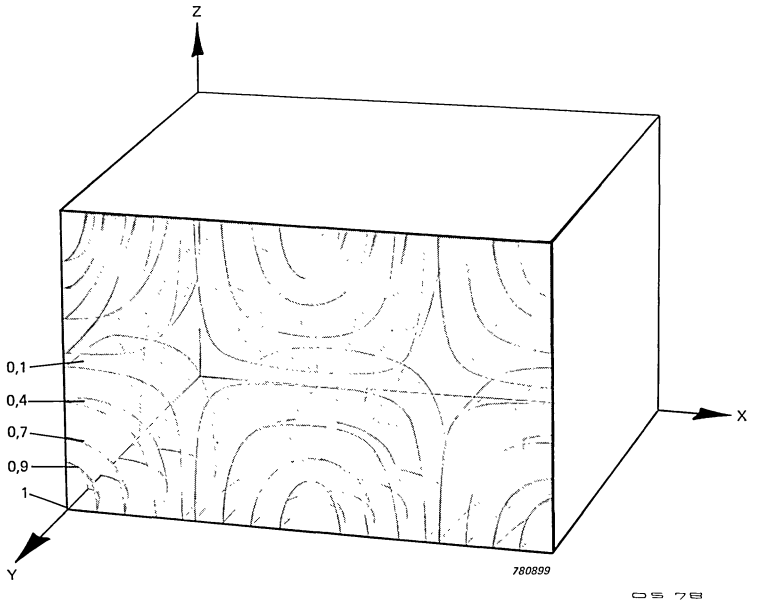

Fig.13. Sound pressure distribution in a rectangular room for the oblique mode (2,1,1). Values are normalized for maximum effective sound pressure P.

The resonant frequency (eigentone) of each eigenmode can be calculated from the formula

$$f_i = \frac{c}{2}\sqrt{\left(\frac{n_x}{l_x}\right)^2 + \left(\frac{n_y}{l_y}\right)^2 + \left(\frac{n_z}{l_z}\right)^2} \qquad [\text{Hz}] \qquad (1)$$

where c is the velocity of sound in m/s
l_x l_y and l_z are the dimensions of the room in m
and n_x n_y and n_z are integers

To evaluate the frequencies for axial modes, two of the ns are set to zero while for tangential and oblique modes one of the ns and none of the ns are set to zero respectively. The number of eigentones of the

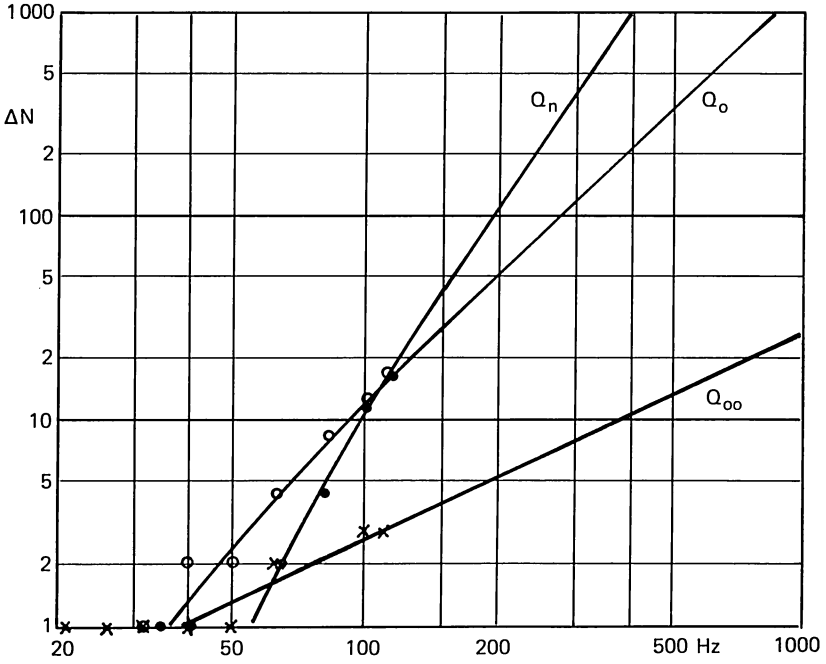

Fig.14. Number of actual eigenmodes in the 240 m³ room in each 1/3 octave band represented by crosses, circles and dots for axial, tangential and oblique modes respectively. The curves are obtained from the abbreviated formulae given in ref.[8]

measurement room lying in 1/3 octave bands are represented by crosses, circles and dots for axial, tangential and oblique modes respectively in Fig.14. It is time consuming to determine the number of eigenmodes using the above formula at higher frequencies as the number of modes increases considerably. However, approximate expressions for determining the number of eigenmodes are derived in Ref.[3] and quoted in Ref.[8] from which Fig.14 is reproduced. It can be seen that the axial and tangential modes dominate at low frequencies while the oblique modes dominate at high frequencies.

In statistical treatment of acoustics, it is assumed that the sound field in the room is diffuse i.e.

a) the energy density in the room is uniform everywhere,
b) the energy flow in all directions is the same and
c) the phase between all waves is random.

The above requirements are fulfilled if there are a large number of eigenmodes in the room, which is the case at high frequencies. At low frequencies, however, the above requirements are not fulfilled and therefore it is necessary to use wave theory instead of statistical theory. In the following the wave theory will be used to explain the curvature in the reverberation decay curves at low frequencies, by treating the eigenmodes in each frequency band individually.

Theory

When a sound source excites a room, forced oscillations are generated, characterised by the spectrum of the sound source and its position in the room. When the sound source is stopped, the oscillation pattern is changed in that only the normal modes of oscillations will now exist in the room. The damping of the oscillations takes place on account of reflections from the walls and to a much lesser extent on account of air damping. The Q factor of the eigenmodes is thus determined by the absorption coefficient of the walls and the mean free path between reflections. As the mean free path is generally longest for the axial modes they will have a longer reverberation time than the tangential and oblique modes.

Mean Free Path

The mean free path for an axial mode can immediately be seen to be the same as the dimension of the room in the direction of the wave.

The general expression for the mean free path ℓ_i for all the three types of eigenmodes is given below and is derived in Appendix B.

$$\ell = \frac{\sqrt{\left(\frac{n_x}{l_x}\right)^2 + \left(\frac{n_y}{l_y}\right)^2 + \left(\frac{n_z}{l_z}\right)^2}}{\frac{n_x}{l_x^2} + \frac{n_y}{l_y^2} + \frac{n_z}{l_z^2}} \qquad [m] \tag{2}$$

Steady State Sound Pressure in a Frequency Band
A monopole sound source emitting white noise with a volume velocity spectral density q [$m^3/s/\sqrt{Hz}$] is rotated in a room. The sound pressure is measured by a rotating microphone away from the source. It is shown in Appendix C that the steady state sound pressure squared in the room for a single eigenmode will be given by

$$p_{i0}^2 = \frac{c^4 q^2 \varrho^2 \pi T_i}{V^2 (\varepsilon_{xi}\varepsilon_{yi}\varepsilon_{zi})^2 \cdot 12 \cdot \ln 10} \qquad [N^2/m^4] \tag{3}$$

where q is the volume velocity spectral density [$m^3/s/\sqrt{Hz}$]
ρ is the air density [kg/m^3]
V is the volume of the room [m^3]
T_i is the reverberation time for the ith eigenmode [s]
ϵ_{xi} ϵ_{yi} and ϵ_{zi} are values depending on the integers for n_x n_y and n_z
ϵ = 1 for n = 0
ϵ = 2 for n > 0

Equation (3) can be written as

$$p_{i0}^2 = C_1 \frac{T_i}{(\varepsilon_{xi}\varepsilon_{yi}\varepsilon_{zi})^2} \tag{4}$$

where $C_1 = \frac{c^4 q^2 \varrho^2 \pi}{V^2 12 \ln 10}$ is a constant

If there are I number of eigenmodes in the frequency band considered, the total RMS sound pressure squared (averaged in time and space) in the frequency band will be given by

$$p_{B0}^2 = p_{10}^2 + p_{20}^2 + \ldots p_{I0}^2 \tag{5}$$

where 0 represents steady state value and p_{10}, p_{20} .. p_{I0} are the sound pressures for the I eigenmodes.

Substituting (4) in (5) we get

$$p_{B0}^2 = C_1 \frac{T_1}{(\varepsilon_{x1}\varepsilon_{y1}\varepsilon_{z1})^2} + C_1 \frac{T_2}{(\varepsilon_{x2}\varepsilon_{y2}\varepsilon_{z2})^2} + \ldots$$

$$\text{i.e.} \quad p_{B0}^2 = C_1 \sum_{i=1}^{I} \frac{T_i}{(\varepsilon_{xi}\varepsilon_{yi}\varepsilon_{zi})^2} \tag{6}$$

Dividing (4) by (6) we obtain

$$\left(\frac{p_{i0}}{p_{B0}}\right)^2 = \frac{\dfrac{T_i}{(\varepsilon_{xi}\varepsilon_{yi}\varepsilon_{zi})^2}}{\displaystyle\sum_{i=1}^{I} \frac{T_i}{(\varepsilon_{xi}\varepsilon_{yi}\varepsilon_{zi})^2}} \tag{7a}$$

As the reverberation time is proportional to the mean free path ℓ_i (see next section) the above equation can also be written as

$$\left(\frac{p_{i0}}{p_{B0}}\right)^2 = \frac{\dfrac{\ell_i}{(\varepsilon_{xi}\varepsilon_{yi}\varepsilon_{zi})^2}}{\displaystyle\sum_{i=1}^{I} \frac{\ell_i}{(\varepsilon_{xi}\varepsilon_{yi}\varepsilon_{zi})^2}} \tag{7b}$$

It can be seen that the steady state sound pressure squared for the individual eigenmodes is proportional to its reverberation time or its mean free path.

Reverberation Time

When the sound source exciting the room is stopped the energy density in each eigenmode will decrease according to the formula

$$D(t) = D_0(1-\alpha)^a$$

$$\text{or} \quad p_i^2 = p_{i0}^2(1-\alpha)^a$$

where D_o is the steady state energy density when t = 0
$D(t)$ is the instantaneous energy density
p_{io} is steady state sound pressure when t = 0
p_i is the instantaneous sound pressure
a is the number of reflections in time t
α is the absorption coefficient of the walls

$$a = \frac{c}{\ell_i} t$$

where c is the velocity of sound
and ℓ_i is the mean free path for the ith eigenmode

Substituting we get

$$p_i^2 = p_{i0}^2(1-\alpha)^{\frac{c}{\ell_i}t} = p_{i0}^2 e^{\frac{c}{\ell_i}t \cdot \ln(1-\alpha)} \quad *$$

$$\text{i.e.} \quad p_i = p_{i0} e^{-\frac{c}{2\ell_i} t \ln\left(\frac{1}{1-\alpha}\right)} \tag{8}$$

When t = T_i (reverberation time), $\frac{p_i}{p_{i0}} = 10^{-3}$

Substituting we get

$$-3 \ln 10 = -\frac{c}{2\ell_i} T_i \ln\left(\frac{1}{1-\alpha}\right)$$

$$\text{i.e.} \quad T_i = \frac{6\ell_i \ln 10}{c \ln\left(\frac{1}{1-\alpha}\right)} \approx \frac{6\ell_i \ln 10}{c \cdot \alpha} \tag{9}$$

for small values of α.

* $\ln x = \log_e x$ and $\log x = \log_{10} x$

The reverberation time can be seen to be proportional to the mean free path and inversely proportional to the absorption coefficient α.

Equation (8) can also be written as

$$p_i \approx p_{i0} e^{-\frac{c}{2\ell_i} t \cdot \alpha} \approx p_{i0} 10^{-\log e \frac{c\alpha}{2\ell_i} t}$$

Substituting equation (9) in the above equation we obtain

$$p_i \approx p_{i0} 10^{-\log e \ln 10 \frac{3t}{T_i}} \approx p_{i0} 10^{-3\frac{t}{T_i}} \qquad (10a)$$

$$\text{i.e. } 20 \log \frac{p_i}{p_{i0}} = -60 \frac{t}{T_i} \qquad (10b)$$

The collective reverberation time of the whole frequency band can now be evaluated. The instantaneous sound pressure squared of the frequency band is given by

$$p_B^2 = p_1^2 + p_2^2 + \ldots p_I^2 \qquad (11)$$

where p_1 ... p_I are the instantaneous values of the RMS sound pressures of each eigenmode at time t

Substituting (10a) in (11) we get

$$p_B^2 = p_{10}^2 10^{-6\frac{t}{T_1}} + p_{20}^2 10^{-6\frac{t}{T_2}} + \ldots + p_{I0}^2 10^{-6\frac{t}{T_I}}$$

Substituting (4) in the above equation we obtain

$$p_B^2 = C_1 \frac{T_1}{(\varepsilon_{x1}\varepsilon_{y1}\varepsilon_{z1})^2} 10^{-6\frac{t}{T_1}} + \ldots + C_1 \frac{T_I}{(\varepsilon_{xI}\varepsilon_{yI}\varepsilon_{zI})^2} 10^{-6\frac{t}{T_I}} \qquad (12)$$

Dividing the above equation by (6) gives

$$\left(\frac{p_B}{p_{B0}}\right)^2 = \frac{\sum_{i=1}^{I} \frac{T_i}{(\varepsilon_{xi}\varepsilon_{yi}\varepsilon_{zi})^2} 10^{-6\frac{t}{T_i}}}{\sum_{i=1}^{I} \frac{T_i}{(\varepsilon_{xi}\varepsilon_{yi}\varepsilon_{zi})^2}} \qquad (13)$$

The above equation illustrates the sound pressure decay of a frequency band with I number of eigenmodes and their respective reverberation times.

Calculation of Reverberation Decay Curves

With the use of the formulae derived above, the reverberation decay curves for each eigenmode and the collective reverberation curves for 63 Hz, 80 Hz and 100 Hz 1/3 octave bands are calculated. As the absorption coefficient α of the walls is not known, the values used are those which give the best correlation between the calculated and the measured decay curves, see "Absorption Coefficient" section under Discussion of Results.

i	n_{xi}	n_{yi}	n_{zi}	$\epsilon_x\epsilon_y\epsilon_z$	f_i [Hz]	ℓ_i [m]	$20 \log \frac{p_{i0}}{p_{B0}}$ [dB]	$\alpha = 0{,}024$ T_i [s]
1	1	2	0	4	58,6	5,11	– 11,3	8,7
2	2	1	1	8	61,6	3,67	– 18,7	6,2
3	0	2	1	4	64,3	4,11	– 12,2	7,0
4	3	0	0	2	65,0	7,85	– 3,4	13,3
5	1	2	1	8	67,9	3,69	– 18,7	6,3
6	0	0	2	2	68,7	4,95	– 5,4	8,4
7	2	2	0	4	69,5	4,89	– 11,5	8,3
8	3	1	0	4	70,4	5,58	– 10,7	9,4

790105

Table 3

In Table 3 the frequencies of the eigenmodes lying in the 63 Hz 1/3 octave band are calculated using eq(1). The mean free path and the relative steady state sound pressure for each eigenmode are evaluated from eq.(2) and (7b) respectively, while the theoretical reverberation times are calculated from eq.(9). The slope of the reverberation curves for each eigenmode can be plotted using eq.(10b) while the start of the reverberation curves are given by the relative steady state levels. The reverberation curves for each eigenmode is thus calculated from the equation

$$20 \log \frac{p_i}{p_{i0}} = -\frac{60}{T_i} t - 20 \log \frac{p_{i0}}{p_{B0}} \qquad (14)$$

and plotted in Fig. 15.

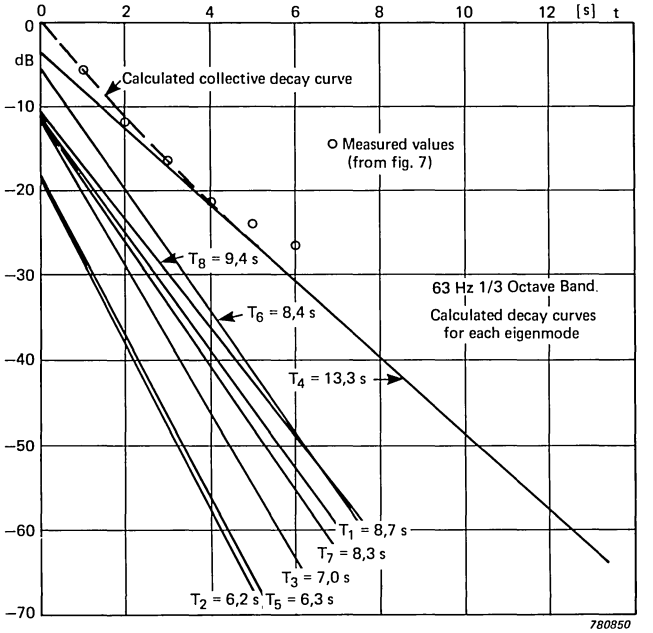

Fig. 15. Calculated decay curves for the 63 Hz 1/3 octave band compared to measured values

The collective reverberation curve for the 1/3 octave 63 Hz band can be plotted either by adding the reverberation curves on energy basis for the eight eigenmodes, or by using eq.(13) and is shown by the dashed line in Fig. 15. The values in Fig. 15 indicated by circles are the actual measured values for the 63 Hz 1/3 octave band and are taken from Fig. 7a.

Eigenmodes		$\epsilon_x \epsilon_y \epsilon_z$	ℓ_i	$10 \log m \left(\frac{p_{i0}}{p_{B0}} \right)^2$	$\alpha = 0{,}026$
Number	Type		[m]	[dB]	T_i [s]
m = 1	axial	2	7,85	− 4,9	12,3
m = 1	axial	2	6,25	− 5,8	9,8
m = 8	tangential	4	4,51	− 4,3	7,0
m = 4	oblique	8	3,74	− 14,1	5,8

790100

Table 4

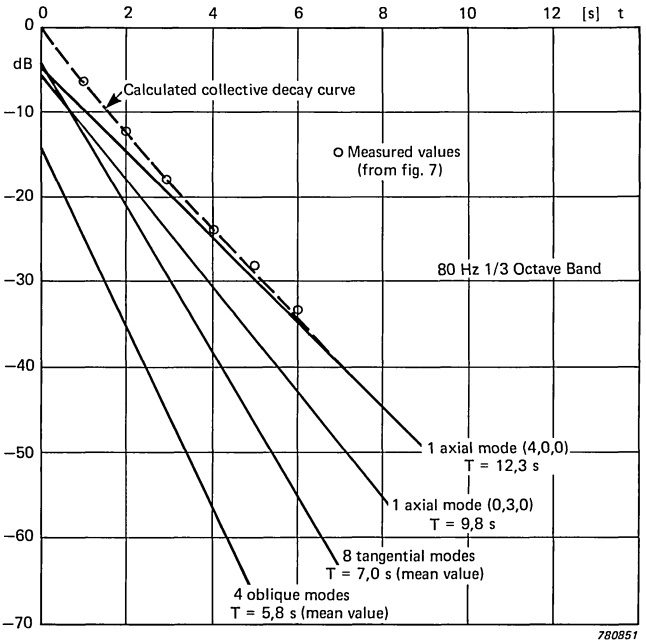

Fig. 16. Calculated decay curves for the 80 Hz 1/3 octave band compared to measured values. The tangential and oblique modes are calculated in groups

Tables 4 and 5 show similar results for the 80 Hz and 100 Hz 1/3 octave bands. As there are a large number of eigenmodes in these frequency bands, the tangential and oblique modes have been grouped se-

Eigenmodes		$\epsilon_x\epsilon_y\epsilon_z$	ℓ_i	$10 \log m \left(\frac{p_{i0}}{p_{B0}}\right)^2$	$\alpha = 0{,}022$
Number	Type		[m]	[dB]	T_i [s]
m = 1	axial	2	7,85	− 6,8	14,5
m = 1	axial	2	6,25	− 7,8	11,5
m = 1	axial	2	4,95	− 8,8	9,2
m = 13	tangential	4	4,87	− 3,8	9,0
m = 12	oblique	8	3,82	− 11,2	7,1

790101

Table 5

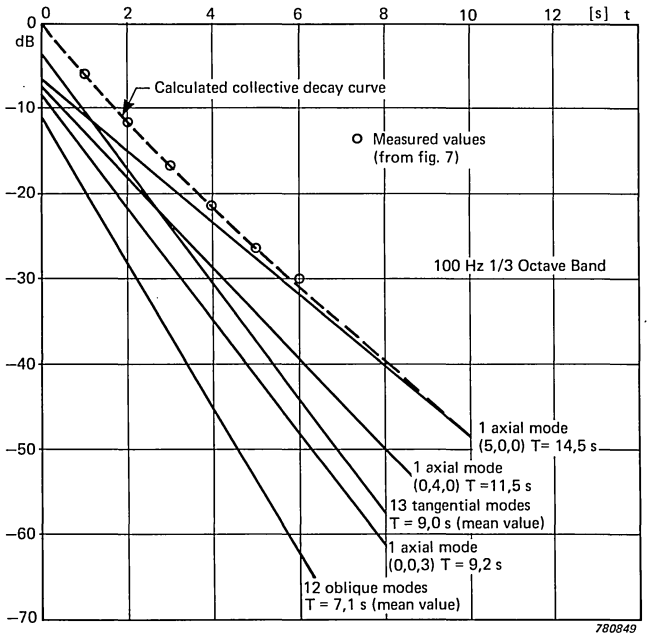

Fig. 17. Calculated decay curves for the 100 Hz 1/3 octave band compared to measured values. The tangential and oblique modes are calculated in groups

parately and the average value of their mean free paths and reverberation times evaluated. The relative steady state sound pressure level for the whole groups have also been evaluated. The reverberation curves for the 80 Hz and 100 Hz 1/3 octave bands are plotted in Figs. 16 and 17 and compared with the measured values.

Discussion of Results

It can be seen from Figs. 16 and 17 that there is good agreement between the calculated and measured results. There is however a principal difference, in that the collective calculated curves have slightly less curvature than the curves obtained from measured results. For the theoretical curves the absorption coefficient is assumed to be independent of the angle of incidence. Fig. 18 which is reproduced from Ref. [3] shows typical curves for the variation of the absorption coefficient as a function of the angle of incidence. The curves are plotted for different

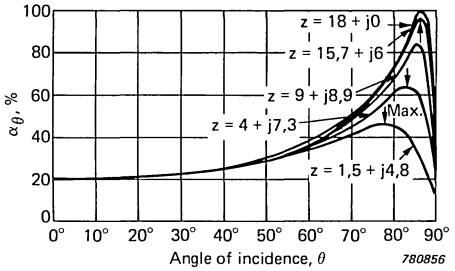

Fig.18. Angle dependence of the absorption coefficient according to the theory of true impedance. The path of glancing incidence, however, is corrected.

values of the acoustic impedance of the wall. 0° refers to normal incidence. The absorption coefficient can be seen to be greater for oblique incidence than for 0° and 90° incidence. This would mean that the axial modes would be less damped and thus have longer reverberation times than calculated while the tangential and oblique modes will have lower reverberation times. As a result there would be better agreement between the calculated and the measured curves.

The agreement is, however, not as good in Fig.15. This could be because the cut-off frequency of the loudspeaker was at 100 Hz and therefore the frequency spectrum was not flat at 63 Hz as assumed. As the level at 63 Hz was also low, the background noise could have had some influence on the measured curve.

From the curves it is evident that the axial modes have a dominating influence on the reverberation decay process. For the 80 Hz frequency band the reverberation curve below the —15 dB level is almost entirely determined by the eigenmode (4,0,0) which corresponds to an axial mode in the direction of the length of the room. Although there are eight tangential modes they have little influence on the reverberation curve while the oblique modes have practically none.

Absorption Coefficient

The absorption coefficients α given in Table 6 have been evaluated using Sabines formula $\alpha = 0{,}161\ V/ST$. The reverberation times used for

Centre frequency [Hz]	63	80	100
α_{sab} (from T measured over 30 dB)	0,013	0,015	0,014
α_{sab} (from early decay time)	0,018	0,019	0,018
α (from table 3,4 and 5)	0,024	0,026	0,022

790102

Table 6

the evaluation have been taken from Fig.8, both for the early decay rate and for the slope between the —5 and —35 dB levels. Also shown in the table are the values assumed for Figs.15, 16, and 17. It can be seen that there are significant differences between the values and is due to the fact that Sabine's equation has been derived using a mean free path of 4V/S. However, the average value of the mean free path will be greater on account of the axial modes dominating at low frequencies. For the room used here 4V/S is equal to 4,08 m. From Tables 3, 4 and 5 the mean values of ℓ can be found to be 4,98 m, 4,65 m and 4,58 m for the 63 Hz, 80 Hz and 100 Hz 1/3 octave frequency bands respectively. Using these values of the mean free path and reverberation time from early decay rate in Sabines formula the absorption coefficient is found to be 0,023, 0,022 and 0,021 in the three bands respectively. These values are close to the values assumed for Figs.15, 16 and 17.

Energy Content in the Eigenmodes

The energy in an eigenmode is given by

$$E = \frac{p^2}{\varrho c^2} V \qquad (15)$$

Substituting eq.(4) in (15) we obtain

$$E = C_1 \frac{T}{(\epsilon_x \epsilon_y \epsilon_z)^2} \cdot \frac{V}{\varrho c^2} \qquad (16)$$

assuming that the sound pressure is averaged over the whole room whilst revolving the source. As $(\epsilon_x \epsilon_y \epsilon_z)^2$ is equal to 4, 16 and 64 for axial, tangential and oblique modes respectively, the energy content for the axial and tangential modes relative to the oblique modes can be calculated.

$$\frac{E_a}{E_o} = \frac{T_a}{T_o} \cdot \frac{64}{4} = \frac{T_a}{T_o} \cdot 16 \qquad (17)$$

$$\frac{E_t}{E_o} = \frac{T_t}{T_o} \cdot \frac{16}{4} = \frac{T_t}{T_o} \cdot 4 \qquad (18)$$

where T_a T_t and T_o are reverberation times for axial tangential and oblique modes respectively.

As $T_a/T_o \approx 2$ the energy content is up to 32 times greater in an axial mode than in an oblique mode, and more than 4 times greater in a tangential mode than in an oblique mode as $T_t > T_o$.

Conclusion

With the use of a Digital Frequency Analyzer Type 2131 and a desk-top calculator it is possible to carry out very accurate reverberation time measurements by averaging with a movable microphone and sound source. The curvature of the reverberation curves at low frequencies is caused on account of the axial modes dominating the last stages of the reverberation process on account of their long reverberation times and high energy content. This has been made clear with relatively simple and approximate calculations of the reverberation process of the individual eigenmodes in a frequency band.

On account of the curvature there is a considerable difference between the reverberation time evaluated over 30 dB (as defined in ISO R 354 and 3382) and that evaluated from the early decay rate upto 500 Hz (see Fig.8) for the measurement room used here.

References

[1] ISO R 354 — Measurement of absorption coefficients in a reverberation room

[2] ISO 3382 — Measurement of reverberation time in auditoria

[3] BRÜEL, P.V. — Sound Insulation and Room Acoustics Chapman & Hall. 1951

[4] KUTTRUFF, H. Eigenschaften und Auswertung von Nachhallkurven, Acustica, Vol.8, 1956

[5] UPTON, R. Automated Measurements of Reverberation Time using the Digital Frequency Analyzer Type 2131. Technical Review No.2—1977

[6] BERANEK, L.L. Noise and Vibration Control. McGraw-Hill 1971

[7] MORSE, P.M. and INGARD, K.U. Theoretical Acoustics. McGraw-Hill 1968

[8] BRÜEL, P.V. The Enigma of Sound Power Measurements at Low Frequencies. Technical Review No.3—1978

[9] RASMUSSEN, K. Noter til forelæsninger i lydfelter. Modul 5105. 1973 Danmarks Tekniske Højskole

[10] KINSLER L.E. & FREY, A.R. Fundamentals of Acoustics. J. Wiley & Sons. 1962

Appendix A

Sound Pressure, Particle Velocity and Energy Density Distribution in a Rectangular Room

From the wave theory of room acoustics ([9] [10] and others) the following formulae are known:

$$|p| = |P \cos k_x x \cos k_y y \cos k_z z| \quad [N/m^2] \tag{A1}$$

where p = effective sound pressure at the point x, y, z N/m^2
P = maximum effective sound pressure (e.g. in a corner) N/m^2
x, y, z are the coordinates from one of the corners in the room m

$$k_x = \frac{n_x \pi}{l_x}, \quad k_y = \frac{n_y \pi}{l_y} \quad \text{and} \quad k_z = \frac{n_z \pi}{l_z} \quad \text{are}$$

wave numbers in the three directions, m^{-1} .
l_x, l_y and l_z are the dimensions of the room, m.
n_x, n_y and n_z are integers n =0, 1, 2 ..

$$|u_x| = \left| \frac{k_x P}{\omega \varrho} \sin k_x x \cos k_y y \cos k_z z \right| \quad [m/s] \tag{A2}$$

$$|u_y| = \left| \frac{k_y P}{\omega \varrho} \cos k_x x \sin k_y y \cos k_z z \right| \quad [m/s] \tag{A3}$$

$$|u_z| = \left| \frac{k_z P}{\omega \varrho} \cos k_x x \cos k_y y \sin k_z z \right| \quad [m/s] \tag{A4}$$

where u_x, u_y and u_z are the particle velocities in the three directions x, y and z respectively m/s
ω = angular frequency rad/s
ρ = density of air kg/m^3

$$D = D_p + D_k \quad [J/m^3] \tag{A5}$$

$$D_p = \frac{1}{2}\frac{|p|^2}{\varrho c^2} \quad [J/m^3] \tag{A6}$$

$$D_k = \tfrac{1}{2}\varrho|u|^2 = \tfrac{1}{2}\varrho(|u_x|^2 + |u_y|^2 + |u_z|^2) \quad [J/m^3] \tag{A7}$$

where D = total energy density
D_p = potential energy density
D_k = kinetic energy density
c = speed of sound in air m/s

Axial modes
For an axial mode in the x-direction:
$n_x > 0, n_y = 0, n_z = 0$ and hence $k_y = 0$ and $k_z = 0$.
From (A1) the sound pressure distribution in the room can be derived:

$$|p| = |P\cos k_x x| = \left|P\cos\frac{n_x\pi}{l_x}x\right|$$

which, for $n_x = 2$ and normalized to P, becomes

$$\left|\frac{p}{P}\right| = \left|\cos\frac{2\pi}{l_x}x\right| \tag{A8}$$

from which the values in Fig. 11b were calculated.

From (A2) the particle velocity distribution in the room can be derived:

$$|u_x| = \left|\frac{k_x P}{\omega\varrho}\sin k_x x\right| = \left|\frac{k_x P}{\omega\varrho}\sin\frac{n_x\pi}{l_x}x\right|$$

which, for $n_x = 2$ and normalized to $U = P/\rho c$ (particle velocity in a free field corresponding to the sound pressure P) becomes

$$\left|\frac{u_x}{U}\right| = \left|\frac{k_x c}{\omega}\sin\frac{2\pi}{l_x}x\right| = \left|\sin\frac{2\pi}{l_x}x\right| \qquad \text{(A9)}$$

as $k_x = k = \omega/c$. From (A9) the values in Fig.11c were calculated.

From (A6) and (A8) the potential energy density is obtained:

$$D_p = \frac{1}{2}\frac{P^2}{\varrho c^2}\cos^2\frac{2\pi}{l_x}x$$

and from (A7) and (A9) the kinetic energy density is:

$$D_k = \frac{1}{2}\varrho U^2 \sin^2\frac{2\pi}{l_x}x$$

which for $U = \frac{P}{\varrho c}$ becomes:

$$D_k = \frac{1}{2}\frac{P^2}{\varrho c^2}\sin^2\frac{2\pi}{l_x}x$$

The total energy density becomes

$$D = D_p + D_k = \frac{1}{2}\frac{P^2}{\varrho c^2}\left(\cos^2\frac{2\pi}{l_x}x + \sin^2\frac{2\pi}{l_x}x\right)$$

$$D = \frac{1}{2}\frac{P}{\varrho c^2} \quad [J/m^3] \qquad \text{(A10)}$$

This means that the total energy density is independent of x as shown in Fig.11d.

Tangential modes

For a tangential mode in the x- and y-directions:

$$n_x>0,\ n_y>0,\ n_z = 0 \text{ and hence } k_z = 0$$

From (A1) the sound pressure distribution in the room can be derived:

$$|p| = |P \cos k_x x \cos k_y y| = \left| P \cos \frac{n_x \pi}{l_x} x \cos \frac{n_y \pi}{l_y} y \right|$$

which for $n_x = 2$ and $n_y = 1$ and when normalized to P becomes

$$\cos \frac{\pi}{l_y} y = \pm \left| \frac{\frac{p}{P}}{\cos \frac{2\pi}{l_x} x} \right| \qquad \text{(A11)}$$

from which the values in Fig.12b were calculated.

From (A2) and (A3) the particle velocity distribution in the room can be derived:

$$u^2 = u_x^2 + u_y^2 = \frac{P^2}{\omega^2 \varrho^2} (k_x^2 \sin^2 k_x x \cos^2 k_y y + k_y^2 \cos^2 k_x x \sin^2 k_y y) \qquad \text{(A12)}$$

which when normalized to

$$U = \frac{P}{\varrho c} = \frac{P}{\varrho} \cdot \frac{k}{\omega} \quad \text{where} \quad k = \sqrt{k_x^2 + k_y^2} \text{ , becomes:}$$

$$\left(\frac{u}{U}\right)^2 = \left(\frac{k_x}{k}\right)^2 \sin^2 k_x x (1 - \sin^2 k_y y) + \left(\frac{k_y}{k}\right)^2 \cos^2 k_x x \sin^2 k_y y$$

from which, for $n_x = 2$ and $n_y = 1$, the following formula can be derived:

$$\sin^2 \frac{\pi}{l_y} y = \frac{\left(\frac{l_x^2}{4 l_y^2} + 1\right) \frac{u^2}{U^2} - \sin^2 \frac{2\pi}{l_x} x}{\frac{l_x^2}{4 l_y^2} \cos^2 \frac{2\pi}{l_x} - \sin^2 \frac{2\pi}{l_x} x} \qquad \text{(A13)}$$

From (A13) the values in Fig.12c were calculated.

From (A1) and (A6) the potential energy density is obtained:

$$D_p = \frac{1}{2} \frac{P^2}{\varrho c^2} \cos^2 k_x x \cos^2 k_y y$$

which together with $\frac{\omega^2}{c^2} = k^2 = k_x^2 + k_y^2$ gives:

$$D_p = \frac{1}{2}\frac{P^2}{\varrho\omega^2}(k_x^2 + k_y^2)\cos^2 k_x x \cos^2 k_y y$$

From $D = D_p + D_k = D_p + \frac{1}{2}\varrho u^2$ and (A12) are obtained

$$D = \frac{1}{2}\frac{P^2}{\varrho\omega^2}\Big[(k_x^2 + k_y^2)\cos^2 k_x x \cos^2 k_y y + k_x^2 \sin^2 k_x x \cos^2 k_y y + k_y^2 \cos^2 k_x x \sin^2 k_y y\Big]$$

$$D = \frac{1}{2}\frac{P^2}{\varrho\omega^2}\left(k_x^2 \cos^2 k_y y + k_y^2 \cos^2 k_x x\right)$$

which normalized to $D_N = \frac{1}{2}\frac{P^2}{\varrho c^2}$ gives:

$$\frac{D}{D_N} = \frac{1}{k_x^2 + k_y^2}\left(k_x^2 \cos^2 k_y y + k_y^2 \cos^2 k_x x\right)$$

from which for $n_x = 2$ and $n_y = 1$ the following formula can be derived:

$$\cos^2 \frac{\pi}{l_y} y = \frac{D}{D_N}\left(1 + \frac{l_x^2}{4l_y^2}\right) - \frac{l_x^2}{4l_y^2}\cos^2 \frac{2\pi}{l_x} x \qquad \text{(A14)}$$

From (A14) the values in Fig. 12d were calculated.

Oblique modes

From (A1) the sound pressure distribution in the room can be derived. Normalized to P and setting $n_x = 2$, $n_y = 1$ and $n_z = 1$ one obtains:

$$\cos \frac{\pi}{l_y} y = \pm \left| \frac{\frac{p}{P}}{\cos \frac{\pi}{l_z} z \cdot \cos \frac{2\pi}{l_x} x} \right| \qquad \text{(A15)}$$

From (A15) the values in Fig. 13 were calculated.

Appendix B

Mean free path between reflections

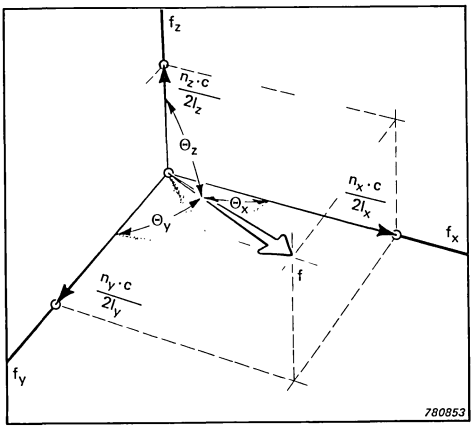

Fig.B1. Frequency vector f in a 3 dimensional rectilinear co-ordinate system

Each eigenmode in a rectangular room can be considered as a vector (f in Fig.B1) in a 3—D co-ordinate system whose origin is one of the corners of the room.

The direction of the vector gives the direction of the sound wave moving in the room with the speed of sound c. If the vector is resolved into three components in the x, y and z directions, the number of reflections in the time t can be determined:

Number of reflections against the y—z walls: $\frac{ct \cos \Theta_x}{l_x}$

Number of reflections against the x—z walls: $\frac{ct\cos\Theta_y}{l_y}$

Number of reflections against the x—y walls: $\frac{ct\cos\Theta_z}{l_z}$

The mean free path ℓ can be expressed as the distance the sound wave moves in the time t divided by the total number of reflections in the same time

$$\ell = \frac{ct}{\frac{ct\cos\Theta_x}{l_x} + \frac{ct\cos\Theta_y}{l_y} + \frac{ct\cos\Theta_z}{l_z}}$$

which together with the following formulae derived from Fig.B1:

$$\cos\Theta_x = \frac{n_x c}{2l_x f}; \quad \cos\Theta_y = \frac{n_y c}{2l_y f}; \quad \cos\Theta_z = \frac{n_z c}{2l_z f}$$

$$\text{and} \quad f = \sqrt{\left(\frac{n_x c}{2l_x}\right)^2 + \left(\frac{n_y c}{2l_y}\right)^2 + \left(\frac{n_z c}{2l_z}\right)^2}$$

$$= \frac{c}{2}\sqrt{\left(\frac{n_x}{l_x}\right)^2 + \left(\frac{n_y}{l_y}\right)^2 + \left(\frac{n_z}{l_z}\right)^2}$$

gives:

$$\ell = \frac{\frac{2f}{c}}{\frac{n_x}{l_x^2} + \frac{n_y}{l_y^2} + \frac{n_z}{l_z^2}}$$

$$\ell = \frac{\sqrt{\left(\frac{n_x}{l_x}\right)^2 + \left(\frac{n_y}{l_y}\right)^2 + \left(\frac{n_z}{l_z}\right)^2}}{\frac{n_x}{l_x^2} + \frac{n_y}{l_y^2} + \frac{n_z}{l_z^2}} \quad [m] \qquad (B1)$$

This formula for the mean free path is valid for axial, tangential and oblique modes.

Appendix C

Calculation of space averaged squared sound pressure for an eigenmode in a rectangular room

For a sound source, radiating sound with a volume velocity, Q_o, at an angular frequency, ω, situated at a point (x_s, y_s, z_s) in a rectangular reverberation room, it can be shown [6] [7] that the RMS sound pressure, p_{io}, measured at point (x_m, y_m, z_m) for **a particular eigenmode, i,** becomes:

$$|p_{i0}(x_s, y_s, z_s, x_m, y_m, z_m)| = \left| \frac{c^2 Q_0 \varrho \omega \Psi_{si} \Psi_{mi}}{V[4\omega_i^2 k_{mi}^2 + (\omega^2 - \omega_i^2)^2]^{\frac{1}{2}}} \right| \quad [N/m^2] \quad (C1)$$

where	c	= speed of sound	m/s
	Q_o	= RMS volume velocity	m^3/s
	ρ	= density of air	kg/m^3
	V	= volume of the room	m^3
	ω_i	= angular resonance frequency for the eigenmode	s^{-1}
	ω	= angular frequency of emitted sound	s^{-1}
	k_{mi}	= decay constant for the eigenmode	s^{-1}

and Ψ_{si} and Ψ_{mi} are the sound pressure distributions for sound source and microphone position respectively. Both quantities are given by:

$$\Psi = \Psi(x, y, z) = \cos\frac{n_x \pi}{l_x} x \cos\frac{n_y \pi}{l_y} y \cos\frac{n_z \pi}{l_z} z \quad (C2)$$

where n_x, n_y and n_z are the integers for the particular eigenmode.

If the sinusoidal volume velocity, Q_o, in equation (C1), is replaced by a volume velocity, q, which has a constant spectral density, (i.e. white noise) then the squared sound pressure for the eigenmode can be expressed by:

$$p_{i0}^2(x_s, y_s, z_s, x_m, y_m, z_m) = \int_0^\infty \frac{c^4 q^2 \varrho^2 \Psi_{si}^2 \Psi_{mi}^2 \omega^2}{V^2(4\omega_i^2 k_{mi}^2 + (\omega^2 - \omega_i^2)^2)} d\omega \qquad (C3)$$

where q = volume velocity spectral density $m^3/s/\sqrt{Hz}$.
Solving the integral we obtain:

$$p_{i0}^2(x_s, y_s, z_s, x_m, y_m, z_m) = \frac{c^4 q^2 \varrho^2 \Psi_{si}^2 \Psi_{mi}^2 \pi}{V^2 4 k_{mi}} \qquad (C4)$$

where it is assumed that $4k_m^2 \ll \omega_i^2$

The space averaged squared sound pressure is obtained by replacing Ψ_{si}^2 and Ψ_{mi}^2 in (C4) by the space averaged values $\overline{\Psi_{si}^2}$ and $\overline{\Psi_{mi}^2}$. These quantities have the same values and can be calculated from:

$$\overline{\Psi^2} = \frac{1}{V} \int_V \cos^2 \frac{n_x \pi}{l_x} x \cos^2 \frac{n_y \pi}{l_y} y \cos^2 \frac{n_z \pi}{l_z} z \, dV \qquad (C5)$$

Solving the integral we obtain:

$\overline{\Psi^2}$ = 1/8 for all ns >0 (oblique modes)

$\overline{\Psi^2}$ = 1/4 for one n = 0 and two ns > 0 (tangential modes)

$\overline{\Psi^2}$ = 1/2 for two ns = 0 and one n > 0 (axial modes)

k_{mi} in (C4) can be replaced by

$$k_{mi} = \frac{3 \ln 10}{T_i} ,$$

where T_i = reverberation time for the mode, i.
The space averaged squared sound pressure is therefore:

$$p_{i0}^2 = \frac{c^4 q^2 \varrho^2 \pi T_i}{12 \ln 10 V^2 (\epsilon_{xi} \epsilon_{yi} \epsilon_{zi})^2} \qquad (C6)$$

where the factors ϵ_{xi}, ϵ_{yi} and ϵ_{zi} have the following values:

ϵ = 1 for n = 0
ϵ = 2 for n > 0

PREVIOUSLY ISSUED NUMBERS OF BRÜEL & KJÆR TECHNICAL REVIEW

(Continued from cover page 2)

4–1974 Underwater Impulse Measurements.
A Comparison of ISO and OSHA Noise Dose Measurements.
Sound Radiation from Loudspeaker System with the Symmetry of the Platonic Solids.

3–1974 Acoustical Investigation of an Impact Drill.
Measurement of the Dynamic Mass of the Hand-arm System.

2–1974 On Signal/Noise Ratio of Tape Recorders.
On the Operating Performance of the Tape Recorder Type 7003 in a Vibrating Environment.

1–1974 Measurements of averaging times of Level Recorders Types 2305 and 2307.
A simple Equipment for direct Measurement of Reverberation Time using Level Recorder Type 2305.
Influence of Sunbeams striking the Diaphragms of Measuring Microphones.

SPECIAL TECHNICAL LITERATURE

As shown on the back cover page Brüel & Kjær publish a variety of technical literature which can be obtained from your local B&K representative.
The following literature is presently available:

Mechanical Vibration and Shock Measurements
(English, German, Russian)
Acoustic Noise Measurements (English, Russian), 2. edition
Strain Measurements
Frequency Analysis (English)
Electroacoustic Measurements
(English, German, French, Spanish)
Catalogs (several languages)
Product Data Sheets (English, German, French, Russian)

Furthermore, back copies of the Technical Review can be supplied as shown in the list above. Older issues may be obtained provided they are still in stock.

PRINTED IN DENMARK . K. LARSEN & SØN A/S . DK-2860 SØBORG

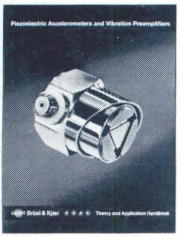

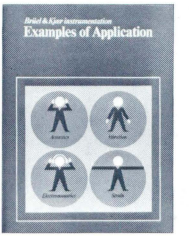

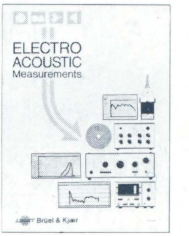

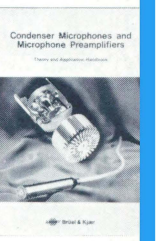

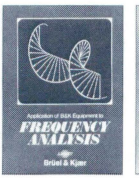

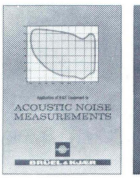

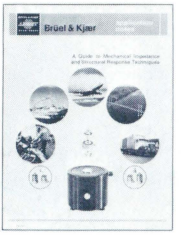

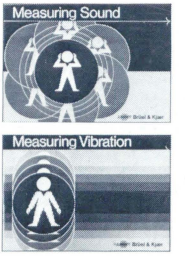

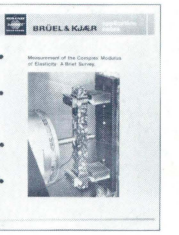

Brüel & Kjær

DK-2850 NÆRUM, DENMARK · Telephone: + 45 2 80 05 00 · Telex: 37316 bruka dk